World Journal of Advanced Engineering Technology and Sciences
eISSN: 2582-8266
Cross Ref DOI: 10.30574/wjaets
Journal homepage: https://wjaets.com/

(RESEARCH ARTICLE)

Check for updates

Climate change and urban flooding in South-South Nigeria from 1990 - 2020

Jeremiah Uriah Richard [1] and Francis Ifeanyi Okeke [2]

[1] *PhD Candidate University of Nigeria Nsukka (UNN).*
[2] *Department of Geoinformatics and Surveying, University of Nigeria Nsukka.*

World Journal of Advanced Engineering Technology and Sciences, 2023, 08(01), 069–089

Publication history: Received on 27 November 2022; revised on 15 January 2023; accepted on 18 January 2023

Article DOI: https://doi.org/10.30574/wjaets.2023.8.1.0013

Abstract

Flooding is one of the disasters that are common in our towns and villages. It occurs as a result of heavy or continuous rainfall over a period of time. Occurrence of flood damages our valuable infrastructure such as buildings, roads, bridges, and schools, churches etc. The study area being a coastal region is confronted with frequent flooding and the extent of damage, and contributing factors has not been fully studied, particularly in applying remote sensing and geographic information system. Also, very little information is known about the combine impacts of urbanization and climate change on urban flooding in the area. Hence this study was aimed at evaluating the impact of climate change and urban development on urban flooding in South – South Nigeria using geospatial techniques. Datasets utilized for the study includes; land use/ land cover derived from Landsat satellite data, soil map, slope model, soil infiltration rate, impervious surface derived from vegetation indices, distance from river, precipitation, and surface temperature data. These datasets were processed into common coordinate system. Landsat data of four epochs (1990 – 2020) was used to map urbanization. Accordingly, the variations in climate variables were investigated using NiMET reported and the satellite derived values. Flood vulnerability zones was determined using multi-criteria analysis implemented in ArcGIS weighted overlay tool. The study observed that urbanization increases from 1990 to 2020, which also increase impervious surfaces, making the area more vulnerable to flooding. In addition, wetland and vegetation cover are being replaced by built-up thereby decreasing the ability of wetland to retained flood water. The lowest rainfall was in 1990 with value 293.70mm and the highest was in 2000 with value 454.90mm. There is general variation of rainfall and temperature from 1990 – 2020 due to climate change. Total built-up at risk was 8873.55ha with most of them situated along the river banks. Geospatial technology is suitable for urban flood vulnerability modeling. For further study, it is recommended that high spatial resolution image should be use to map trends in urbanization. In addition, drainage density should be integrated in flood vulnerability modeling.

Keywords: Climate Change; Flood; Google Earth Elevation; Multi-criteria Analysis; Slope Model; Temperature; VSWI

1. Introduction

Globally, urbanization is a continuous process in most towns and cities. Our towns and cities are expanding in response to increase in population and economic activities. United Nations, (2014) stated that as at 2014, over 54 percent of the world population is urban dwellers.Urbanization in Nigeria may be traced by experts to the period of oil boom in the early 1970s, couple with massive improvement in roads and availability of vehicles for transportation. Also, it is believed that as at 1986 urban population growth rate in Nigeria increase to 6 percent per year. Jaysawal and Saha, (2014) defined urbanization as the transformation from traditional rural economies to a modern industrial cities. It is mostly caused by a number of factors and some of them are; industrial growth, job opportunities, improved technology and improved living conditions (Pawan, 2016). Generally, urbanization is associated with lots of negative effects (Hillman, 2013). Peculiar in many urban areas is urban flooding. Urban flood can be caused by urban development, climate change, and population increase (Kaspersen et al, 2016).

*Corresponding author: Jeremiah Uriah Richard

IPCC, (2012) defined climate change as the state of the climate which can be identified by changes in the mean or the variability of its properties that persists for an extended period, usually decades. Climate change is caused by the accumulation of greenhouse gases such as CO_2, N_2O, and CH_4 (WHO, 2008). In addition, other greenhouse gases are ozone, and water vapour (UNISDR, 2009). Climate change main driver is the anthropogenically released carbon dioxide (CO_2) into the atmosphere (Union of Concerned Scientists, 2012). Greenhouse gases increased global temperature by 1.3 degrees (F) over the last century and with the expectation to warm by 2 to 11 degrees in 2100 (National Wildlife Federation, 2009). In Texas, for example, the temperature has increase by one degree (F) in the past century (EPA, 2016). Climate change has brought about uneven temperature and precipitation globaaly and the degree of impact varies from one geographical location to the other.

Climate change has a major impact on floods and it is believed to have caused immense havoc worldwide. Studies have shown that floods menace has affected both developed and underdeveloped countries either directly or indirectly. FEMA 480, (2005) defined flood as the general and temporal condition of partial or complete inundation of normally dry land areas. Its occurrence is caused by either anthropogenic or natural sources (National Institute of Urban Affairs, 2016). Floods impacts can be rural or urban in nature (NOAA, 1992). Flooding is a common phenomenon in most towns and cities in the world, causing significant damage to people, the economy and the environment. Floods, when occurs, can affect airports, rail lines, roads, water supplies, electricity, and sewage systems (WHO, 2008). Flood water which is usually polluted is accompanied by different kinds of diseases, insects and organisms. Floods lead to waterborne diseases such as hepatitis A, leptospirosis, giardiasis, dermatitis, and conjunctivitis as reported by experts. It disrupt power supply, telecommunications lines, obstruction of cities traffic, destruction of aquatic organisms, and pollution of ground and surface water (Rain Community Solution, 2017). Floods risk may be direct or indirect on the impacted areas. Direct impact may be catastrophic compared to the indirect impact.

Climate change-related flood cases have been recorded in different parts of the globe. For instance, the rainstorm leading to severe flood in the UK on December 5^{th}- 6^{th} was caused by climate change (Friends of the Earth, 2015). In the United States, heavy rainfall has been on increase since 1950s due to changing climate (Forbes and Christina, 2014). The increase in rainfall was severe in the northeast and Midwest respectively. Climate change impact also increases the intensity of rainfall causing landslides, floods, and droughts during the summer in Asia (UNFCCC, 2007). Landslides arising from floods were experienced in Edo State, South-South Nigeria in 2017, leading to the collapse of buildings, roads, and fences.

Floods disaster has been studied by many researchers using known models and approaches. For example, Muhammad and Iyortim, (2013) used three datasets (high-resolution image, field interview observation, and Digital Terrain Model (DEM) to studied flood impacts in the middle course of Kaduna River, Nigeria. Their studies only considered flood impacts and not climate change related.

Here, the evaluation of impacts of climate change and urban development on urban flooding was analyzed using MCA by integrating climate variables, DEM and other datasets in a GIS environment to model urban flood vulnerability areas in relation to climate change.

The objectives of the study are; (a) To determine the change in land use/ land cover from 1990 – 2020 as a result of urbanization.(b) To assess the spatial variability of climate extremes (land surface temperature and precipitation) from 1990 – 2020 and their effects on urban flooding. (c) To determine flood vulnerable area using multi-criteria evaluation in ArcGIS 10.1 software. (d) To determine critical features at risk from the vulnerability map due to urban flooding.

1.1. Study Area

The study area is a section of Rivers and Bayelsa State,Nigeria, located on longitude 6° 25’50”E - 6° 39’45”E and latitude 5° 12’20”N - 4° 55’15”N in the World Geodetic System 1984 (WGS84). The study area is part of the Niger Delta and also part of the Gulf of Guinea. It has a total area of 74357ha. The rock types are sedimentary in nature depicting that of the Niger Delta region of Nigeria (Youdeowei and Nwankwoala, 2016) and the geology has been classified into Akata and Agbada petroleum systems (Tuttle et al, 1999). The three main soil types in the study area according to Nigeria soil map are nitisols, ferralsols, and gleysols. It has two main seasons (wet and dry season). Wet season is associated with rainfall while the dry season is associated with harmattan. Generally, rainfall in Nigeria is controlled by the moist northward maritime air-mass that blew from the Atlantic Ocean and the continental air-mass that blew southward from the African landmass (National Bureau of Statistics, 2010). Raining season started from March to October while dry season started from November to February every year (Uko and Tamunobereton-Ari, 2013). The 2009 annual precipitation and temperature as reliably reported by NiMET was 2,601.6mm and 23.2°C (National Bureau of Statistics, 2010). Notable land use in the area include; built-up including both residential and industrial, agricultural farmlands and roads

including the popular east-west road, major roads, main paths, and track roads. Land cover are earth's surface features that exist naturally and they include; rivers, creeks, streams, mangrove swamps, topography, and vegetation. The study area was selected due to repeated flood menace in 2017, 2018 and 2020 causing range of impacts on political, socio-economic and cultural life of the people. Secondly, the rapid urbanization of the region due to industrial activities associated with oil exploration by the multi-national companies. The region hosts about two dozen International Oil Companies (IOCs) (Francis et al, 2011).

The study area map is as shown in figure 1.

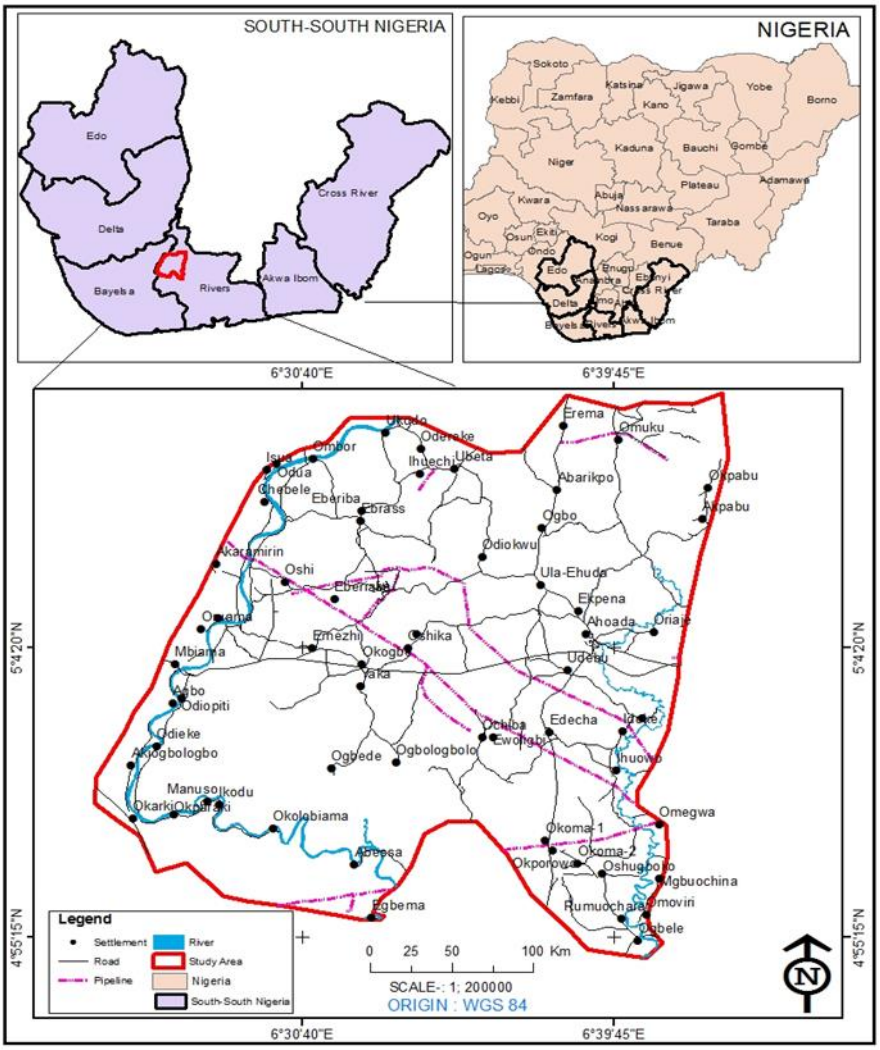

Figure 1 Study area map in red with south-south and Nigeria as insets

2. Methodology

2.1. Dataset and Software

Landsat imageries used for the study were obtained from its website (http://glovis.usgs.gov/). Landsat data was selected for the study because it can be downloaded free-of-charge. The images were downloaded using path 188 and row 57 which contained metadata file. The selected Landsat were the precision orth-corrected product (LIT) that has been corrected for radiometric and geometric distortions (USGS, 2017). The soil map was obtained from the Nigeria soil map. It was collected from the Office of the Surveyor-General of the Federation (OSGOF) – data clearinghouse in Nigeria. Also included in the flood analysis was digital elevation model (DEM0 obtained from Google Earth (GE) elevation. The elevation data was extracted using GPS Visualizer link http://www.gpsvisualizer.com/convert_input. Other datasets used in the study are; Land Surface Temperature (LST) obtained from NiMET and satellite derived, precipitation data downloaded from its website (http://www.tamsat.org.uk) free-of-charge, population data collected from the National

Population Commission (NPC), and settlement data collected from OSGOF.Other datasets needed for the study were derived from these datasets. Table 1 summarized the characteristics of the datasets used and Table 2 also provides details of the Landsat datasets used in the urban flood study.

Table 1 Summary of datasets used in the study

Data	Date	Resolution (m)	Source
Landsat Imageries	1990 - 2020	30 x 30/ 60 x 60	http://glovis.usgs.gov/
DEM	2/11/2016	NA	Google Earth
Soil Map	NA	NA	FUGRO
Temperature	1990 - 2020	30 x 30	http://glovis.usgs.gov/
Precipitation	1990 - 2020	NA	http://www.tamsat.org.uk
Settlement	NA	NA	OSGOF
Population	NA	NA	NPC

Table 2 Landsat datasets and their characteristics used in the study

Sensor	Path/ Row	Imagery Date	Resolution (m)	Source
Landsat MSS	189/ 56	02/12/1990	60 x 60	http://glovis.usgs.gov/
Landsat ETM	189/ 56	30/05/2000	30 x 30	http://glovis.usgs.gov/
Landsat ETM	189/ 56	02/01/2010	30 x 30	http://glovis.usgs.gov/
Landsat OLI	189/ 56	06/01/2020	30 x 30	http://glovis.usgs.gov/

Software used for flood mapping are; ESRI's ArcGIS 10.1, ENVI 5.0, Statistical Package for the Social Sciences (SPSS), and PANCROMA™. Each of the software was used to performed specific task.

2.2. Data Processing

2.2.1. Land use/ land cover

Radiometric enhancement was performed on the image prior to analysis to improve its pictorial quality (Richards and Jia, 2006). Also, periodic line dropout in the image data was also corrected. The periodic line dropout resulted in gaps on the image data and was corrected using PANCROMA ™ (John, 2012). In May 31, 2003, Landsat image developed gaps (missing data) due to failure of the Scan Line Collector (SLC) (Landsat Technical Guide, 2004, Pat et al, 2004). The only one with gap is the 2010 image which was corrected using another 2010 image of different acquisition date. Prior to image classification, band combinations were formed from three bands (green, red and infrared). These band combination is simply refers to as false colour composite. For OLI image 2020, green is band 3, red is band 4 and infrared corresponds to band 5 (USGS, 2016). The bands were selected for urban land use change analysis. Band 5 4 3 is ideal for vegetation interpretation. In this study supervised classification method was used to extract land use/ land cover categories. Supervise image classification required the selection of training sites. The minimum numbers of independent training pixel required is N + 1, where N is the number of spectral band (Richards and Jia, 2006). The image classification method adopted was maximum likelihood classification (MLC). It was chosen base on its accuracy level (Richards and Xiuping, 2006) also applied MLC in the classification of remote sensing image. The study adopted level 1 classification scheme to extract land use/ land cover types (Anderson et al, 1976). The land use/ land cover types classified includes; water body, built-up, vegetation, and wetland. Classification accuracy of the remotely sensed data was also computed. It is crucial because of the infiltration of errors from various sources. Lu and Weng, (2007) listed such errors as include classification, interpretation errors, poor quality of training sites, and positional errors. Accuracy assessment can be represented using error matrix (Congalton, 1991). In this study, thematic map accuracy was presented based on overall accuracy and kappa statistics.

2.2.2. Rainfall data

Rainfall over the area was obtained from the Tropical Applications of Meteorology using Satellite data and ground-based observations (TAMSAT) data. Downloaded TAMSAT data with an extension PNG (University of Reading, 2017) was georeferenced using geographic coordinates as appeared on the maps border. The maps were georeferenced in ArcGIS 10.1 software with a root mean square errors (RMSEs) ranging from 0.00002 to 0.00033. Shapefile was created to extract spatial distribution of rainfall values in millimeters.

2.2.3. Land surface temperature

Is defined as the temperature at a particular point on the earth's surface (Rebecca and Russell, 2013). It can be estimated by land-based and the remote sensing-based methods. Large area coverage, ability to estimate temperature in inaccessible locations and cost effective is the advantages of remote sensing method. It was derived from Landsat satellite imageries. The bands used for the study are band 6 which is the thermal band for Landsat TM and ETM+ (Centre for Biodiversity and Conservation, 2004) and band 10 which is also thermal band for Landsat OLI (USGS, 2016). The low gain thermal band (band 6-1) was used for the Landsat ETM+.In addition, band 6 of TM has 120m x 120m spatial resolution (Anji, 2008; Richards and Xiuping, 2006) while band 10 of OLI image has 100m x 100m resolution (USGS, 2016), but these bands were resampled to 30m x 30m resolution by the data provider prior to data download. In deriving surface temperature, the satellite images were converted from digital numbers (DNs) to top of atmosphere (TOA) radiance. TOA radiance ideally represents the actual reflectance from the earth's surface features. Digital numbers (DNs) is a dimensionless unit which does not represents any physical quantity (Abduwasit, 2010) and as such required conversion. Kumar et al, (2012) derived surface temperature from LANDSAT ETM+ by first converting DNs to TOA radiance as specified in LANDSAT guide. The transformation of DNs to TOA and the computation of surface temperature follow the formulae expressed in the LANDSAT user's guide.

For the LANDSAT Thematic Mapper (TM), and Enhanced Thematic Mapper Plus (ETM+), TOA radiance in $Wm^{-2}Sr^{-1}$, is computed using the formula,

$$L_\lambda = (LMAX_\lambda - LMIN_\lambda)/ QCALMAX - QCALMIN \times (DN - QCALMIN) + LMIN_\lambda \text{ ---------- } 1$$

Where,
$LMAX_\lambda$, = maximum spectral radiance for the band
$LMIN_\lambda$ = minimum spectral radiance for the band
QCALMAX = maximum quantize calculated for the band
QCALMIN = minimum quantize calculated for the band
DN = pixel DN value (Abduwasit, 2010).

For LANDSAT OLI, TOA radiance is computed using the formula,

$$L_\lambda = M_L \times Q_{cal} + A_L \text{ ----------2}$$

Where,
L_λ = spectral radiance in $Wm^{-2}Sr^{-1}$
M_L = radiance multiplicative scaling factor for the band
Q_{cal} = L1 pixel value in DN and
A_L = radiance additive scaling factor for the band (USGS, 2016).

The surface temperature was computed from the TOA radiance image using the formula,

$$T = \frac{K2}{\ln\left(\frac{K1}{L\lambda}+1\right)} \text{ ----------3}$$

Where,
T = TOA brightness temperature in Kelvin
L_λ = spectral radiance in $Wm^{-2}Sr^{-1}$
K1 and K2 are the thermal conversion constant for band 6 and 10. The parameters M_L, A_L, K1, and K2 are obtained from the Landsat header file.

2.2.4. Vegetation Supply Water Index (VSWI)

It was used to map impervious surface (IS) of urban area.Kent et al, (2002) defined impervious surface (IS) as area within a watershed that is cover by non-infiltrated surfaces. Other researchers defined it as a surface that prohibits the infiltration of water from the land surface into the underlying soil. Asad et al, (2017) used normalized difference built-up index (NDBI) and Wei and Blaschke (2014) used spectral mixture analysis and object base image analysis classification to map IS. VSWI was developed by Carlson et al, 1990 and is given by the formula,

$$VSWI = \frac{\text{NDVI}}{\text{Ts}} \text{----------4}$$

Where,
VSWI = Vegetation supply water index
NDVI = Normalized Difference Vegetation Index
Ts = remote sensing image estimated brightness temperature expressed in Celsius scale.

From the VSWI equation, lower value indicates the presence of drought and higher values indicates absence of drought.

2.2.5. Soil map

Soil map was georectified in other to transform to known coordinate system. The three soil classes: Ferrasols, located in the north-east. Nitisols found in the south-east and Gleysols covering the greater part of the map was extracted. Soil data was assigned Curve Number (CN) to each category before transformed to raster data format. Curve Number was adopted by Soil Conservation Service (SCS) and used in hydrology for predicting soil rate of infiltration (Rincon et al, 2018).

2.2.6. Soil Infiltration

Also called soil sealing. Infiltration is defined as the downward entry of water into the soil (Johnson, 1991). The rate at which rainwater flows through the soil layers is measure by infiltration rate in inches per hour. The movement of water varies from texture to texture. Large pores as in sandy soil allows rainwater to drain easily through it than clay soil with small pores and highly compacted (USDA-NRCS, 2004). The imperviousness of urban areas will increase runoff with the resultant flooding. Accordingly, within urban, the impacts of flooding increases especially when there were no enough drainage systems to discharge runoff (Anni et al, 2020; Martinez et al, 2019). Soil infiltration rate of various soil textures has been developed. These values may be easily applied to soil data in geographic information system (GIS) to determine infiltration for the soil unit. The study adopted Hillel, (1982) infiltration values of various soil types. Table 3 summarized soil infiltration rate in inches per hour (in/hr) of different soil textures.

Table 3 Soil infiltration rates in inches per hour

Soil type	**Infiltration rate (in/hr)**
Sand	>0.8
Sandy and silty soils	0.4 – 0.8
Loam	0.2 – 0.4
Clayey soils	0.04 – 0.2
Sodic clayey soils	<0.04

2.2.7. Slope Model

Slope is defined as the steepness or gradient of a unit of terrain expressed as an angle in degrees or as a percentage (Heywood et al, 2006). Slope is used to measures the rate of change at a chosen point on the surface. According to Zhilin et al, (2005) slope model is an important DTM surface widely used to represent terrain descriptors (hills, mountains, ridges, roads, buildings, etc). In addition, slope may be easily calculated on a DTM surface. Slope equation according to Heywood et al, (2006) is given by the formula;

$$S = b^2 + c^2 \text{ ----------5}$$

Where,

S = slope
b, c = constants whose values are determined from the equation of best fit using 3 x 3 window on DTM surface given by the equation;

$$z = a + bx + cy \text{ ----------6}$$

Where,
z = height at the point of interest
x, y = coordinates of point at the centre
a, b, c = constants.

Slope may be generated using GIS software like ESRI's ArcGIS, SURFER, ArcHydro etc. and it is being used in many applications areas like surface and sub-surface hydrology. Chanthanmas et al, (2017) had used slope as input data in a multi-criteria evaluation to map flood hazard zones in Kolliaris River basin and Thailand.

The slope value was produced in degrees with the default nine (9) classes.It was reclassified from the default nine (9) classes to five (5) classes as required in the analysis.

2.3. Multi-criteria Analysis (MCA)

Decision making is the responsibility of everybody, group or organization. Decisions may be complex (requiring critical thinking and applications of software) or simple (requiring simple ideas) in nature. Multi-criteria analysis is one of the methods aim at resolving complex decisions, especially, one relating to the environment. Multi-Criteria analysis is a tool to assist decision makers in arriving at solutions to conflicting problems (Lesslie et al, 2008). It is needed in solving numerous real life problems (Marimuthu and Ramesh, 2015). The operations of MCA may be applied to both non-spatial and spatial environmental problems. Spatial MCA transformed geographical data into output map that are used in making decisions (Joshi and Shahapure, 2015). The conflicting decisions are actualized using Analytic Hierarchy Process (AHP) developed by Thomas Saaty (Saaty, 1977).

Flooding is one of such complex decision, requiring MCA approaches. Solutions to flooding usually required an integrated approach, including the application of GIS-based MCA. GIS-based MCA supports the integration of multiple datasets for making accurate decisions on flooding. In practice, many researchers have applied GIS-based MCA to model flood risk and vulnerability in different areas. Lawal et al, (2012) used MCE to study flood vulnerability areas in Malaysia. Yahara, (2008) applied GIS MCA to study flood vulnerability in Hadejia-Jama'Are River Basin, Nigeria.

Implementing GIS-based MCA requires three elements namely; factors, scales and weights. The factors utilized in modeling flood vulnerability includes; land use/ land cover map, soil map, rainfall data, slope model, IS, distance to river and surface temperature. These factors which are in raster data formats were reclassified and ranked according to its influence in the decision making.

2.4. Population at Risk

The population at risk due to flood disaster was derived from the population of each settlement in the area. The population provided by national population commission (NPC) was that of 1991 that has been archived at community level (CL). The latest population was still at the local government level (LGL) and cannot be utilized for analysis of flood risk. Population of 1991 was used to project to the current date population by applying projection factors provided by the commission. The population was projected using the annual growth rate (AGR) in 2006 and 2020 respectively. Population projection according to NPC is computed using the equation;

$$P_p = P_l (1 + (A/100 \times N)) \text{ ----------7}$$

Where;
P_p = Projected population to a given date
P_l = Last Population count
A = Annual growth rate
N = Number of years projected into the future

Annual growth rate is a factor introduced by NPC base on country's growth rate of that particular year. In this study, NPC recommended AGR of 2.9 and 3.4 for 2006 and 2020 respectively were utilized in the population projection.

3. Results and discussion

3.1. Urban Development

There is evidence of urbanization in the area due to increase in built-up from 1990 to 2020. In 1990 urbanization stood at 2564.19ha which is 3.45 percent of the total area, but by 2000 it increases to 10677.15ha representing 14.38 percent of the area. Accordingly, urbanization in 2010 was 10784.76ha which represents 14.52 percent of the total area, but in 2020 urbanization increases to 11001.96ha representing 14.82 percent of the total area. Urbanization leads to soil compaction caused by construction activities (Leopold, 1968). Also, the increase in urbanization created impervious surfaces within the built-up and also increase the frequency of flood disaster. As urbanization increases other land cover which serves as reservoir for flood water are being destroyed for construction purposes, paving ways for flood damage. Loss of wetlands and vegetation cover due to urbanization was responsible for flooding. Wetland decreases in 1990 from 28044.90ha to 17723.52ha in 2020. Richard and Abah, (2020) in their study observed depletion of wetland from 2000 to 2013 by 13.52 percent in Port Harcourt.Wetland function is to protect urban areas from flooding (Tiffany et al, 2006) but when they are depleted the severity of urban flooding increase. This was revealed in the 2020 flood disaster in this part of south-south with many towns and villages completely submerged by flood water. It was seen as the worst flood in history. In south-south Nigeria several construction are on the increase on the available wetlands and vegetation by the multi-national companies. Wetlands in south-south are being reclaimed by the multi-national companies for the expansion of exploration activities in the region thereby creating more flood prone zones in the area. In addition, wetlands and vegetation that can reserve flood water are continually cleared for the construction of buildings, roads, and industrial base by these multi-nationals. Figure 2 a-d is the classification maps of 1990 – 2020.

The reclamation of coastal communities in the south-south by the Niger Delta Development Commission (NDDC) also leads to loss of wetlands capacity to retain flood water. When wetlands are reclaimed the capacity to hold water is no longer guaranteed and during heavy downpour location that hitherto not flooding becomes flooded. The reclamation of Tombia in Degema Local Governemnt Area, Rivers State and Kula in Akuku-toru Local Governemnt Area, Rivers State, South-South Nigeria is perfect examples of wetland degradation by NDDC.

Besides loss of wetlands, urbanization can also leads to global warming. During construction heat energy are radiated to the atmosphere leading to global warming (increase in green house gasses). Green house gases are among the factors causing climate change which in turn influences urban flooding. In South-South Nigeria the observable increase in urbanization may in turn influenced the incidence of climate change which may results to increase precipitation. Table 4 represents area in hectares of land use/ cover classification.

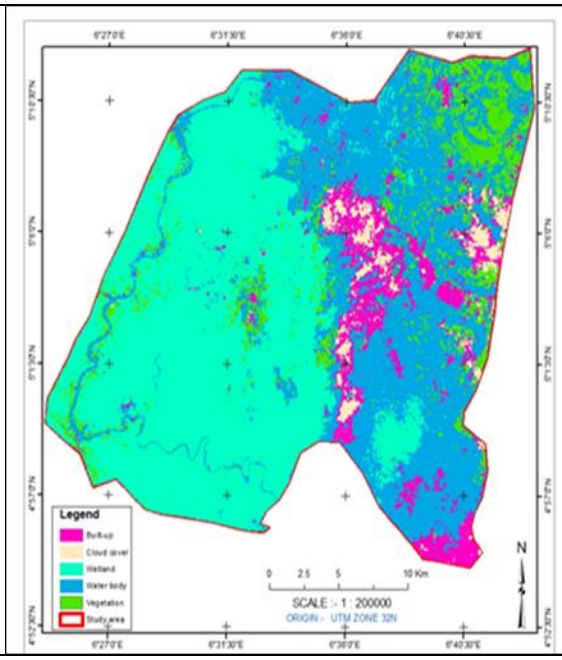

(a) Classification map 1990

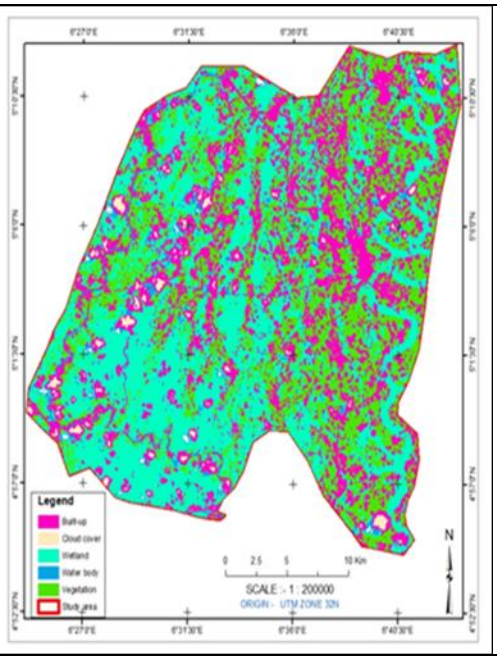

(b) Classification map 2000

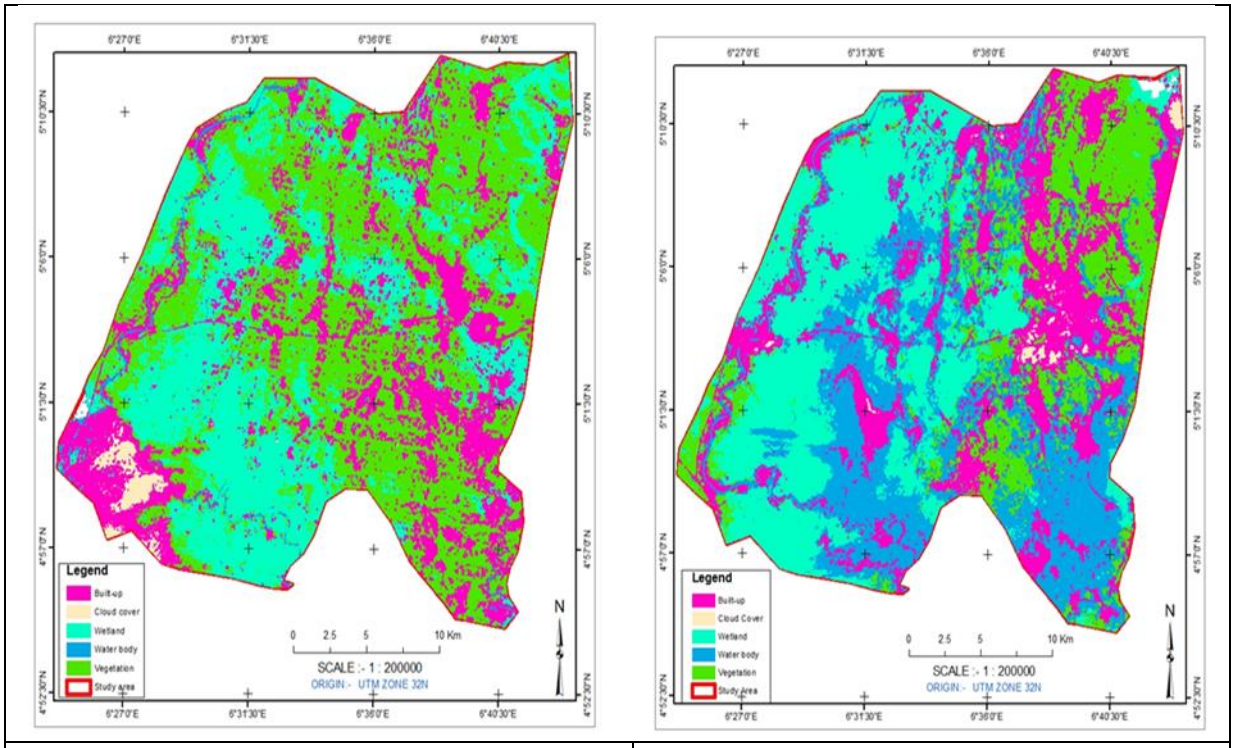

(c)Classification map 2010 | (d) Classification map 2020

Figure 2 a – d are the classification maps from 1990 – 2020

Table 4 Total area per class in land use/ land cover calculated in hectares

Lulc Type	1990		2000		2010		2020	
	Area (ha.)	% (ha.)	Area (ha.)	% (ha.)	Area (ha.)	% (ha.)	Area (ha.)	% (ha.)
Built-up	2564.19	3.45	10677.15	14.38	10784.76	14.52	11001.96	14.82
Cloud cover	2240.01	3.02	1584.09	2.13	1222.65	1.65	856.71	1.15
Wetland	28044.90	37.77	21641.31	29.14	17922.37	24.14	17723.52	23.87
Water body	23799.24	32.05	2752.83	3.71	23536.40	31.70	23196.51	31.24
Vegetation	37159.65	23.85	21378.69	50.04	20776.62	27.98	17707.77	28.79
Total	74256.75	100	74256.75	100	74256.75	100	74256.75	100

The changes were rapid from 1990 to 2000, but become steady from 2000 to 2020. Urban expansions continuously replacing other land cover thereby paving the ways for flood risk (Umaru and Adedokun, 2020). Changes in built-up was also represented using bar chart as shown in figure 3.

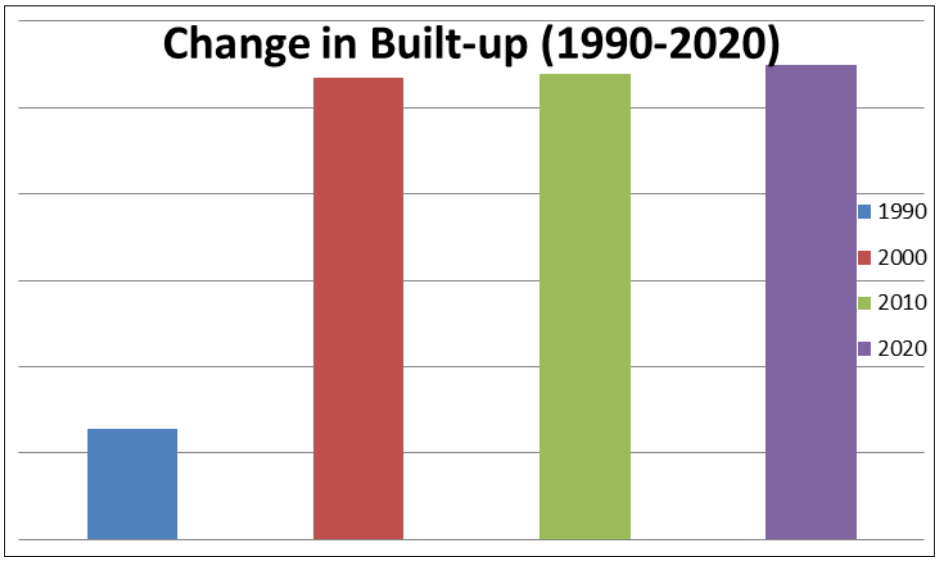

Figure 3 Bar chart showing changes in built-up from 1990 – 2020

3.2. Spatial Variability of Precipitation and Temperature

Figure 4 is the line graph of NiMET observed surface temperature from 1990 to 2020. The line graph shows steady increase in temperature from 1990 to 2020, giving rise to a straight line graph. The line graph is very close to the axis origin. The results presented in the graph shows that temperature increase to 3.20°C within thirty (30) years (1990 – 2020). Also, there is a slight increase in temperature between 1990 and 2000 (10years) by just 0.20°C. This supported Haider, (2019) that climate change impact has increase temperature by 0.2 to 0.3°C per decade in most region of the country. Accordingly, World Bank Group, (2021) also reported 0.19°C increase per decade. But within three (3) decades (30years) in the region, the increase was alarming, indicating strong signal in the region. Such an increase in temperature will impact negatively on the environment. The impact may not be limited to flooding alone but also to agricultural sectors (Haider, 2019). In summary, there is a general increase in temperature in the region drive by climate change.

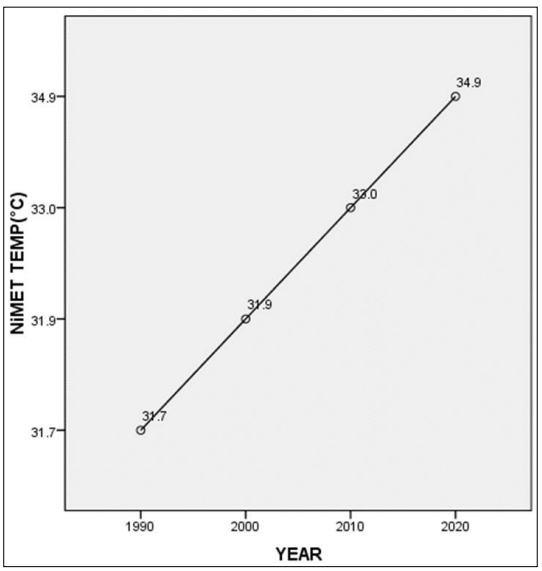

Figure 4 Line graph of NiMET observed temperature against the years

Similarly, figure 5 graphically depicts trend in NiMET precipitation from 1990 to 2020. The line graph shows reduce rainfall in 1990 but increase to 454.90mm in 2000. Later in 2010 it reduces from that to 454.10mm and in 2020, rainfall drops to 430.10mm. Similarly, for the satellite derived rainfall it was same in 1990, 2000 and 2020, but in 2010 it

dropped significantly to 500mm which is very close to the NiMET data in that same year. Line graph of NiMET observed is shown in figure 5.

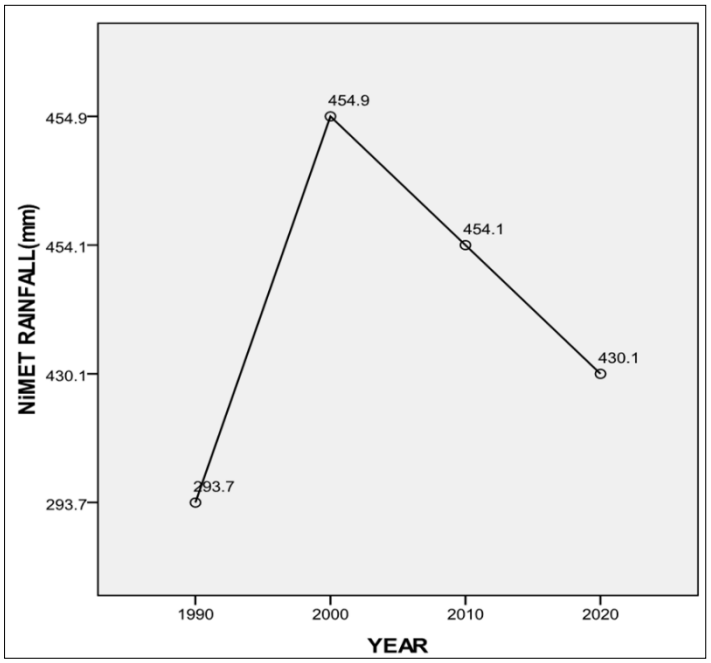

Figure 5 Line graph of NiMET rainfall against the study years

The fluctuation in rainfall from 1990 to 2020 was in response to climate change phenomenon which resulted to flooding (Haider, 2019). Also, it is directly responsible for the variations in monthly and yearly flooding of communities. In addition, the peak rainfall mostly occurred in the month of September and the flooding experienced arises from the accumulated rainfall from other months that could not be absorbed by the soil. In other worlds, the soil has gotten to it stress limit.

3.3. Modeling Flood Vulnerable Zones

The parameters for the flood vulnerable zones analysis were all processed into raster data formats and ranked according to their importance in the model. The inverse ranking method (Yahaya, 2008) was adopted to rank all the factors in the decision making process. The inverse ranking method assigned higher value to factor that is highly vulnerable to flooding and lowest value to least vulnerable to flooding.

Land use/ cover were reclassified into four classes using reclassify tool in ArcGIS. Built-up was assigned rank of 4 being most vulnerable to flooding and water body ranked 3. Water body is the source of flooding to most towns and villages but lacks the capacity to impact on itself rather on other land use/ cover. Wetland and vegetation ranked 2 and 1 respectively. During flooding most wetlands are susceptible to flooding than the adjoining vegetation with lesser flood impacts. Criteria and the reclassified map used in the analysis are shown in figure 6a- n.

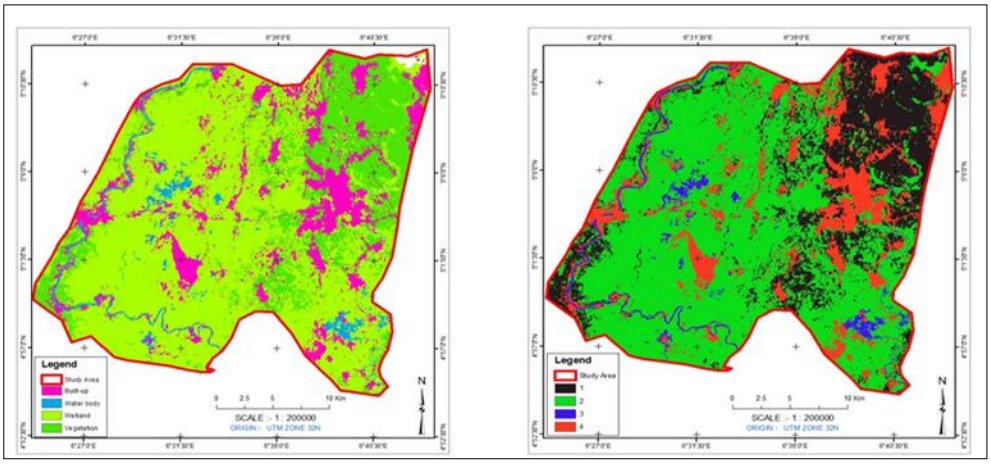

(a) Land use/ cover map (b) Reclassed land use

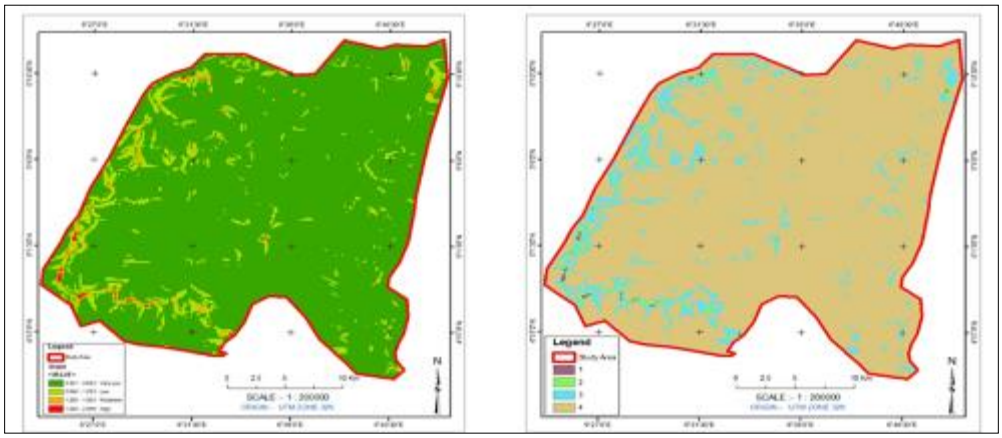

(c)Slope (d) Reclassed slope

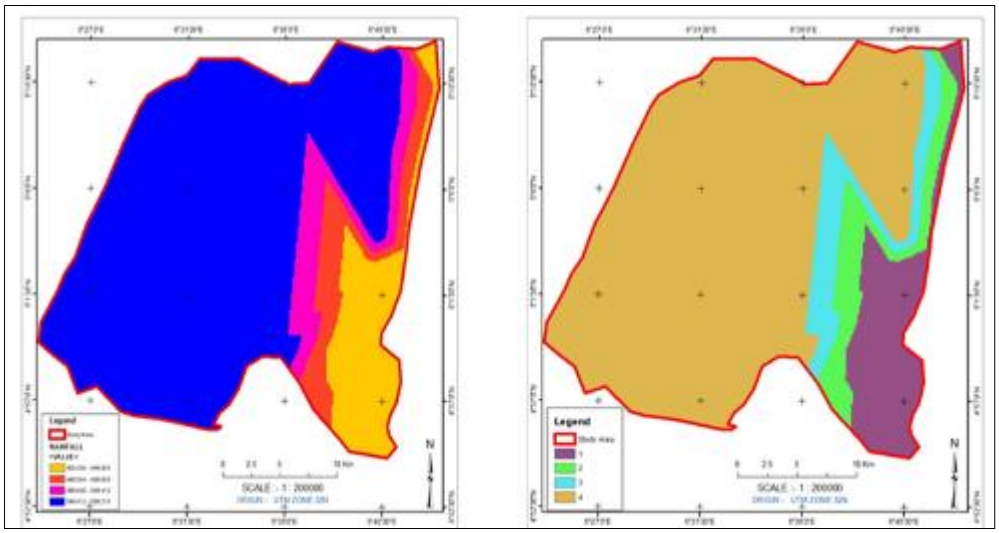

(e)Rainfall (f) Reclassed rainfall

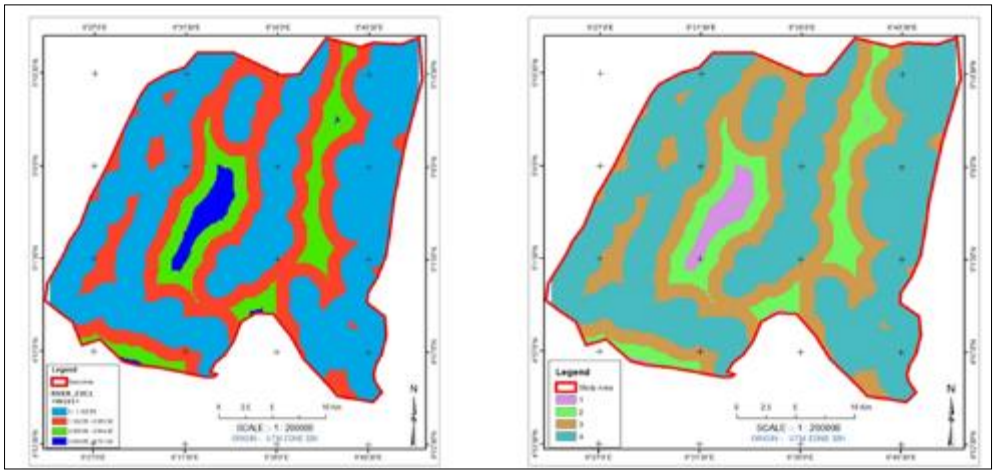

(g)Distance to river (h) Reclassed distance to river

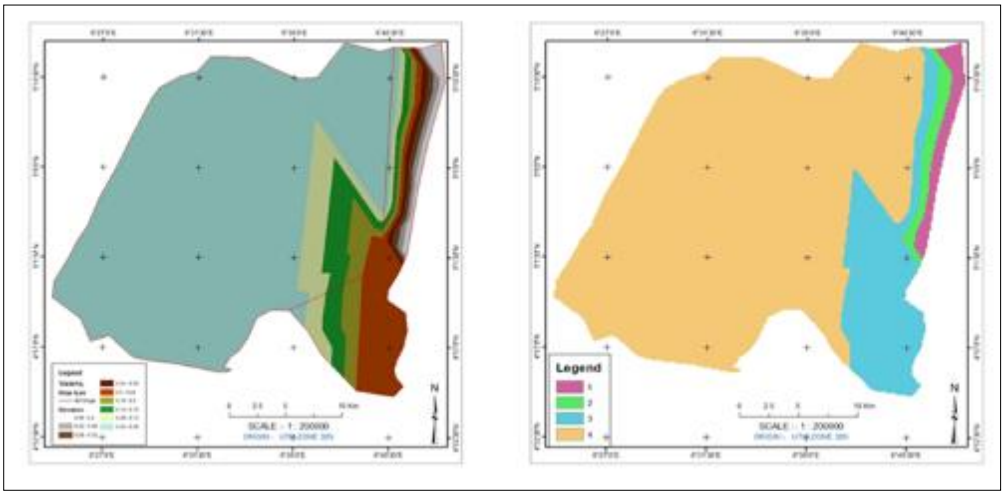

(i)Soil Infiltration (j) Reclassed soil infiltration

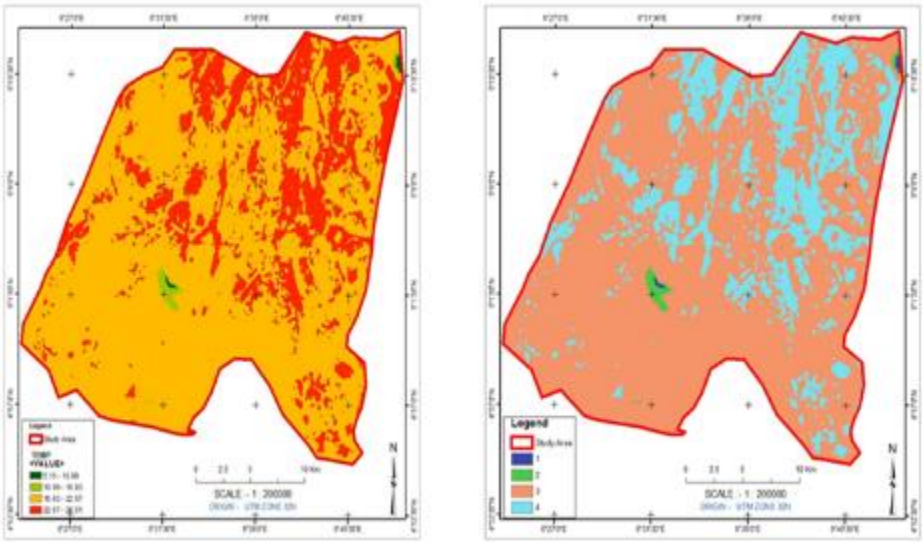

(k) Surface temperature (l) Reclassed temperature

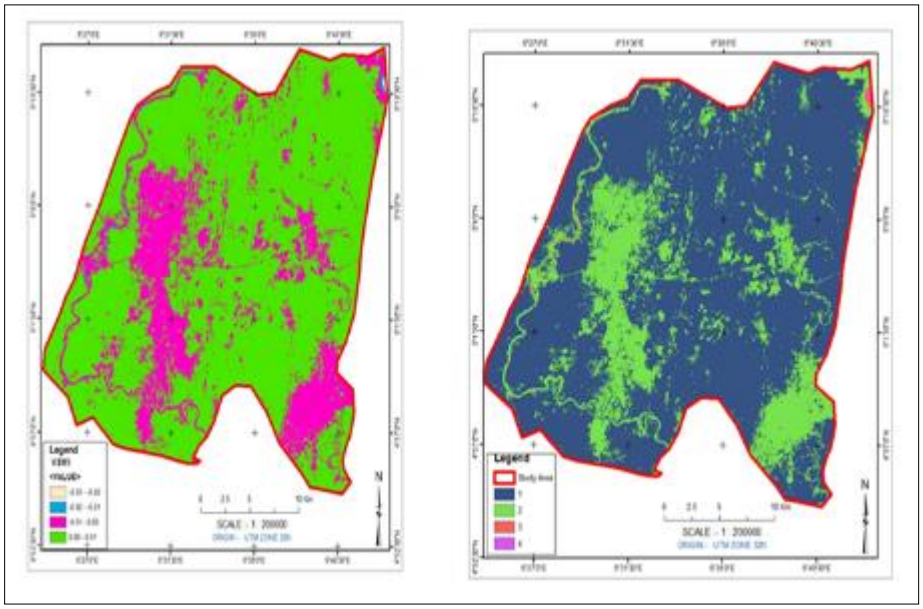

(m)Impervious surface (n) Reclassed impervious surface

Figure 6a - n Criteria and the reclassed maps used in multi-criteria analysis

For the model to work effectively, the percentage influence for each factor was assigned to all the reclassified datasets. Percentage influence determine the influence of the factor in the decision making (ESRI's, 2008). Higher the percentage of influence, the more important the factor in the decision making process.

In this study, Land use/ land cover was assigned percentage influence of 30, precipitation 20, soil 10, slope 5, land surface temperature (LST) 5, distance from river 10, impervious is 10 and infiltration rate is 10. The total percentage influence required for the flood vulnerability model to optimally work is 100 and it was strictly adhere to in the analysis.

These factors and their ranges are shown in table 5. The table also specified the requirement for flood vulnerability. In the table, the factors were ranked from the highest 4 to the least 1.

Table 5 Factors and percentage influence used in modeling flood vulnerable zones

S/n	Factors	rank/ range		Risk	% influence
1	Land Use/Cover	4	Built-up	Very High	30
		3	Water body	High	
		2	Wetland	Moderate	
		1	Vegetation	Low	
2	Temperature (°C)	4	22.674 – 28.514	Very High	5
		3	16.834 – 22.674	High	
		2	10.994 – 16.834	Moderate	
		1	5.154 – 10.994	Low	
3	Rainfall (mm)	4	549.412 – 599.216	Very High	20
		3	499.609 – 549.412	High	
		2	449.804 – 499.608	Moderate	
		1	400.000 – 420.753	Low	
4	Slope (°)	4	0.001 – 0.642	Very High	5

		3	0.642 – 1.283	High	
		2	1.283 – 1.925	Moderate	
		1	1.925 – 2.566	Low	
5	VSWI (Impervious)	4	-0.022 - -0.012	Very High	10
		3	-0.012 - -0.002	High	
		2	-0.002 – 0.008	Moderate	
		1	0.008 – 0.018	Low	
6	Soil	4	82.500 – 100.000	Very High	10
		3	65.000 – 82.500	High	
		2	47.500 – 65.000	Moderate	
		1	30.000 – 47.500	Low	
7	Distance From River (km)	4	0.000 – 1.183	Very High	10
		3	1.163 – 2.366	High	
		2	2.366 – 3.549	Moderate	
		1	3.549 – 4.732	Low	
8	Soil infiltration rate (inch/hr)	4	0.040 – 0.130	Very High	10
		3	0.130 – 0.220	High	
		2	0.220 – 0.310	Moderate	
		1	0.310 – 0.310	Low	

Figure 7 is the urban flood vulnerability map produced from weighted overlay tool in ESRI's ArcGIS. The three vulnerability classes are low, moderate and high vulnerable represented by different colours.Low vulnerability class is found more in the east and was represented in solar yellow. It has a total area of 10201.39ha, representing 13.88% of the total area and the area of the minimum and maximum polygons are 1.56ha and 8130.64ha respectively. Some of the settlements that are located in the low vulnerable zones are Ihuowo, Okoroma 1 and 2, Oshogboko, Akpabu and Ogbele.

The second class was the moderate vulnerability zone represented with chrysoprase green. They occur mostly in the wetland and vegetation which adjourned built-up. The total area of the moderate zone was 57257.27ha and covering the greater portion of the map. The area of the minimum and maximum class polygons are 1.56ha and 56038.04ha respectively. Moderate vulnerability zone represent 77.90% of the total area, indicating great danger in flood risk.

The third class was the high urban flood vulnerability zone represented by mars red. The minimum and maximum areas are 1.56ha and 532.09ha and the total area was 6047.39ha representing 8.23% of the area. The vulnerable zones are located along the Orashi River in the west and very few along Sambreiro River in the east. Umaru and Adedokun, (2020) has also observed that settlements alone River Benue in Kogi State are highly susceptible to flood disaster. In most cases, the degree of impact depends on the proximity to the river. Some of the settlements that are located in the high vulnerable zones are Akinima, Mbiama, Oshi, Okarki, Odieke, Odiopiti, Odereke, Odua, Ekpena and Ahoada. Vishwanath and Tomaszewski, (2018) corroborated this study that settlements are the most susceptible to flooding.The result was not validated as there were no existing data on extent of flood vulnerability in the study area.

Soil characteristic contributed to the vulnerability of the area. Highly vulnerable zone are located within the neighbourhood of gleysols.This soil type is associated with high water table and low infiltration rate. According to Hillel, (1982) gleysols has infiltration rate ranges from 0.04 – 0.2in/hr. In addition, highly vulnerable zone are surrounded by wetland which are also susceptible to flood. These wetlands also have boundaries with the Orashi River – a popular fresh water river in the area. Flooding was those from the wetland, river and the runoff from the excess water due to impermeable surfaces created by urbanization. Flood vulnerability map showing the three vulnerable zones is shown in figure 7 and the class area and percentage of the area is display in table 6.

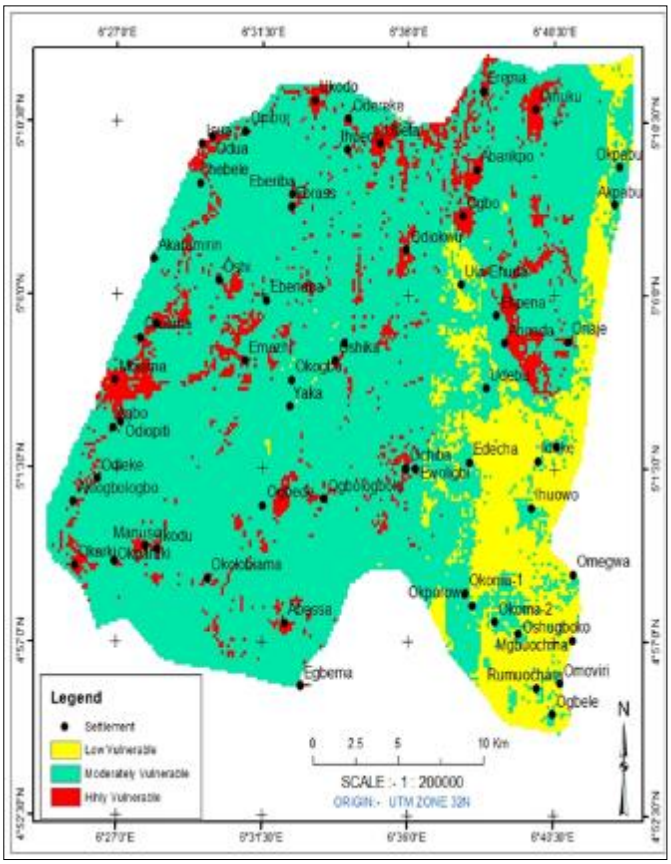

Figure 7 Urban flood vulnerability map

Table 6 Urban flood vulnerability class and area

CLASS	AREA(ha)	% AREA	MIN(ha)	MAX(ha)
Low	10201.39	13.88	1.56	8130.64
Moderate	57257.27	77.90	1.56	56038.04
High	6047.39	8.23	1.56	532.09
Total	73506.05	100		

3.4. Modeling Features at Risk

Built-up that are at risk of urban flood were produced using the high vulnerable flood zones to clip all the built-up that are covered by the zones. The clipped built-up were converted to geodatabase from which the total area was computed. Total built-up at risk due to urban flood was 8873.55ha with most of them situated along the river banks. Figure 8 is the built-up at risk due to urban flood menace in the study area.

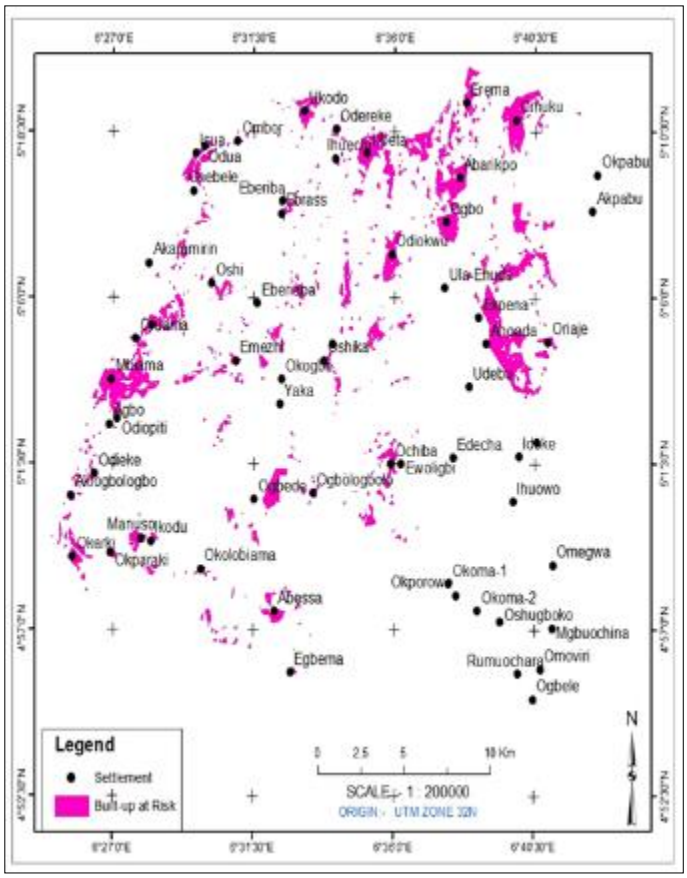

Figure 8 Built-up at risk due to urban flood disaster

Population at risk during flood disaster was model using population data obtained from NPC. The projected 2020 population was used. The total population of male and female affected in Akinima was 7,333, Mbiama was 6,619, Oruama was 1,591 and 7,744 in Odiereke. Also, it was 11,293 in Okarki, 3,366 in Ogbede and 624 in Odiopiti. Vishwanath and Tomaszewski, (2018) has shown that 65 percent features at risk of flood disaster is population. The 2020 flood disaster completely submerged Mbiama, Okarki and Akinima. They are among the major towns in the local government area and these population and other valuables were affected. Mbiama market is an international market and during the flood menace, the market was shutdown. The flood height in the community was above one (1m), forcing residents to desert their homes. Also in Okarki, the flood level was close to the window level in some locations in the town and some above window level. Their farmland was completely submerged, causing scarcity of food stuffs in the area.

Figure 9 is the bar chart representing 2020 population of some selected settlements that are at risk of flood water. The bar chart was produced using SPSS software with the population on the vertical axis and settlements on the horizontal axis. From the chart, Okarki has the highest populations (male and female) that are at risk and it was followed by Akinima. The lowest population at risk was Akaramirin with a population of 911. Some of the settlements are situated close to a river or wetland which is liable to flood and as such become flooded during downpour.

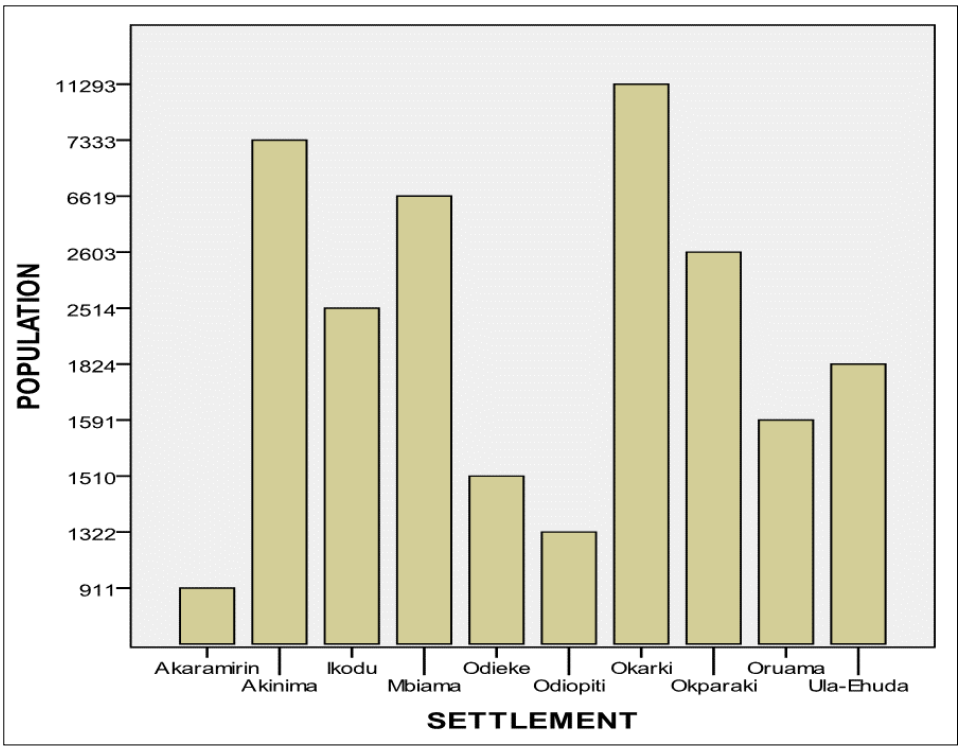

Figure 9 Bar chart showing 2020 population at risk due to flood disaster

4. Conclusion

Flooding is one of the natural disasters ravaging towns and cities all over the globe. Flood was first recorded in the holy bible when Almighty God destroyed the whole earth. Some floods are caused by the overflow of water channels during heavy downpour while others are triggered by the blockage of drainages within an urban environment. Like the natural flood, all floods are associated with varying degrees of impacts. Little has been done on the combine impacts of urbanization and climate change on flood disaster in the region by integrating geospatial data derived from various sources. This study evaluates the impacts of climate change and urban development on urban flooding in study area using geospatial technology. The study applied remote sensing data and GIS software to analyze all the datasets needed in the evaluation of the combined impacts on flooding. The study observed that urbanization increases from 1990 to 2020 and the increase in urbanization contributed to flooding. Secondly, climate change variables are fluctuating from year to year as observed in the study. There is a general increase in climate variable. Finally, vulnerable zones and population at risk was mapped using geospatial technology. It is recommended that further study should consider sea level rise (SLR) and ground water flood.Also, establishment of weather stations in all local government area may significantly improve the estimations of climate variables which may further advance our study.

Compliance with ethical standards

Acknowledgments

Let me appreciate my dear wife Mrs. Ruth Jeremiah for her supports during this thesis. May I also thank my colleagues Jonah Iyowuna, Adekule Ibrahim and Andrew Abah for their collectives supports during the programme. My special thanks to my supervisor Prof. F. I. Okeke for his role in my work. Finally, my appreciations to all the staff of the University for their service to me during my studies.

Disclosure of conflict of interest

The authors involved in this articles have unanimously agreed and declared that no conflict of interest with anybody or group.

References

[1] United Nations, (2014). World Urbanization Prospects the 2014 Revision, Department ofEconomic and Social Affairs, New York, pp. 1-32.

[2] Jaysawal, N. and Saha, S. (2014). Urbanization in India: An Impact Assessment, InternationalJournal of Applied Sociology, Vol. 4, No. 1, pp. 60-65.

[3] Pawan, P. (2016). Urbanization and its Causes and Effects: A Review, International Journal ofResearch and Scientific Innovation (IJRSI), Vol. III, No. IX, pp. 110-112.

[4] Hillman, B. (2013). The Causes and Consequences of Rapid Urbanization in an EthicallyDiverse Region: A Case Study of a County Town in Yunnan, China Perspectives, pp. 26-32.

[5] Kaspersen, P. S., Drews, M., Arnbjerg-Nielsen, K., & Madsen, H. (2016). Impacts of urbandevelopment and climate change in exposing cities to pluvial flooding. Technical University of Denmark (DTU), pp. 1-49.

[6] IPCC, (2014). Annex II: Glossary [Mach, K.J., S. Planton and C. von Stechow (eds.)]. In: Climate Change 2014: Synthesis Report. Contribution of Working Groups I, II and III to the Fifth Assessment Report of the Intergovernmental Panel on Climate Change [Core Writing Team, R.K. Pachauri and L.A. Meyer (eds.)]. IPCC, Geneva, Switzerland, pp. 117-130.

[7] WHO, (2008). Floods: Climate Change and Adaptation Strategies for Human Health, Report ona WHO Meeting, London, United Kingdom, pp. 1-52.

[8] UNISDR, (2009). Terminology on Disaster Risk Reduction, United Nations InternationalStrategy for Disaster Reduction (UNISDR) Geneva, Switzerland, pp. 1-35.

[9] Union of Concerned Scientists, (2012). After the Storm: The Hidden Health Risks of Flooding ina Warming World, Climate Change and your Health, Two Brattle Square, Cambridge, MA 02138-3780, pp. 1-24.

[10] National Wildlife Federation, (2009). Increase Flooding Risk: Global Warming's Wake-up Callfor Riverfront Communities, pp. 1-12, WWW.NWF.ORG/EXTREMEWEATHER

[11] EPA, (2016). Climate Change Means for Texas, EPA 430-F-16-045, pp. 1-2.

[12] FEMA 480, (2005). National Flood Insurance Program (NFIP) Floodplain ManagementRequirements. A Study Guide and Desk Reference for Local Officials – FEMA480, pp. D-4. https://www.financialwatchngr.com/2016/09/19 flood-destroys-12-homes-rivers-state/.

[13] National Institute of Urban Affairs, (2016). Urban Flooding, India-Urban Climate Change FactSheets, pp. 1-6.

[14] NOAA, (1992). Flash Floods and Floods, the Awesome Power, a Preparedness Guide. U.S.Department of Commerce, National Oceanic and Atmospheric Administration, National Weather Service, pp. 1-12.

[15] Rain Community Solution, (2017). Urban Flooding in Ontario, Toward Collective ImpactSolutions, Discussion Paper Draft 2.0, 416 Chambers Street, Second Floor Peterborough Ontaria K9H 3V1, pp. 1-44.

[16] Friends of the Earth, (2015). Floods, Climate Change and Flood Defence Investment, See ThingsDifferently, pp. 1-7.

[17] Forbes, T., and Christina, D. (2014). Heavy Precipitation in the U.S. and the Climate ChangeConception, World Resources Institute, Fact Sheet, pp. 1-6.

[18] UNFCCC, (2007). Climate Change: Impacts, Vulnerabilities and Adaptation in DevelopingCountries, United Nations Framework Convention on Climate Change, Martin-Luther-King-Strasse 853175 Bonn, Germany, pp. 1-68.

[19] Muhammad, I., and Iyortim, O. S. (2013). Application of Remote Sensing (RS) and GeographicInformation Systems (GIS) in Flood Vulnerability Mapping: Case Study of River Kaduna, International Journal of Geomatics and Geosciences, Vol. 3, No. 3, pp. 618-627.

[20] Youdeowei, P. o., and Nwankwoala, H. O. (2016). Analysis of Soil and Sub-Soil PropertiesAround Veritas University, Obehie, Southeastern Nigeria, African Journal of Engineering Research, Vol. 4, No. 1, pp. 6-10. pp. 25-30.

[21] Tuttle, m. L. W., Charpentier, R., R. and Brownfield M. E. (1999). The Niger Delta PetroleumSystem: Niger Delta Province, Nigeria, Cameroon, and Equatorial Guinea, Africa, USGS Open- File Report 99-50-H, pp. 6.

[22] National Bureau of Statistics, (2010). Annual Abstract of Statistics, Federal Republic of Nigeria,pp. 4.

[23] Uko, E. D. and Tamunobereton-Ari, I. (2013). Variability of Climate Parameters in PortHarcourt, Nigeria, Journal of Emerging Trends in Engineering and Applied Sciences, Vol. 4, No. 5, pp. 727 – 730.

[24] Francis, P., Lapin, D. and Rossiasco, P. (2011). Securing Development and Peace in the NigerDelta, a Social and Conflict Analysis for Change, One Woodrow Wilson Plaza, 1300 Pennsylvania Ave, Washington, DC 20004, pp. 6.

[25] USGS, (2017). LEDAPS Product Guide Version 7.6, pp. 1-35.

[26] Richards, J.A., and Xiuping, J. (2006). Remote Sensing Digital Image Analysis, 4th Edition,Springer-Verlag Berlin Heidelberg, Germany, pp.397, 393.

[27] John C. (2012). PANCROMATM Satellite Image Processing Making Satellite BetterTM,Instruction Manual Version 101, pp. 1-399, www.PANCROMA.com.

[28] Landsat Technical Guide, (2004). Global Land Cover Facility, University of Maryland Institutefor Advanced Computer Studies, Department of Geography, http://ltpwww.gsfc.nasa.gov/IAS/handbook/handbook_toc.html, pp. 1-2.

[29] Pat, S., Esad, M., and Gyanesh, C. (2004). SLC Gap-Filling Products Phase One Methodology,pp. 1-5.

[30] USGS, (2016). Landsat 8 (L8) Data Users Handbook, Version 2.0, Department of the Interior,U.S. Geological Survey, pp. 9.

[31] Anderson, J. R., Ernest, E. H., John, T. R., and Richard, E. W.(1976). A Land Use and LandCover Classification System for Use with Remote Sensor Data, Geological Survey Professional Paper 964, a Revision of the Land Use Classification System as Presented in U.S. Geological Survey Circular 671, pp. 1–41.

[32] Lu, D., and Weng, Q. (2007). A Survey of Image Classification Methods and Techniques forImproving Classification Performance, International Journal of Remote sensing, Vol. 28, No. 5, pp. 823-870.

[33] Congalton, R. G. (1991). A Review of Assessing the Accuracy of Classifications of RemotelySensed Data, Remote Sen. Environ, vol. 37, pp. 35-46.

[34] University of Reading, (2017). TAMSAT Data Policy, pp. 1-3.

[35] Rebecca, L. D. and Russell, G. C. (2013). Meeting Environmental Challenges with RemoteSensing Imagery, American Geosciences Institute, 4220 King Street, Alexandria, VA 22302, USA. www.agiweb.org. pp. 44.

[36] Centre for Biodiversity and Conservation, (2004). Remote Sensing & Geographic InformationSystems Facility, American Museum & Natural History, pp.1-16.

[37] Anji, M. R. (2008). The Textbook of Remote Sensing and Geographic Information Systems,3rd Edition, 4-4-309, Giriraj Lane, Sultan Bazar, Hyderabad-500 095-A.P, p92.

[38] Abduwasit, G. (2010). Calculating Surface Temperature using Landsat Thermal Imagery, Macelwane Hall 324 3507 Laclede Ave, St Louis, MO 63103, pp. 1-9.

[39] Kumar, S. K., Bhaskar, P. U., Padmakumar, K. (2012). Estimation of Land Surface Temperatureto Study Urban Heat Island Effect using Landsat ETM+ Image, International Journal of Engineering Science and Technology, Vol. 4, No. 2, pp. 771-778.

[40] Kent, B. B., John, M. M., and Martin C. R. (2002). Impervious Surfaces and the Quality ofNatural and Built Environments, Department of Geography and Environmental Planning, Towson University, 8000 York Road Baltimore, Maryland 21252-0001, pp. 1-28.

[41] Asad, M. Ahmad, S. R., Ali, F., Mehmood, R., Butt, M. A. and Rathore, S. (2017). Use ofRemote Sensing for Urban Impervious Surfaces:A case Study of Lahore, International Journal of Engineering and Applied Sciences (IJEAS), Vol. 4, No. 8, pp. 88-92.

[42] Wei, C. and Blaschke, T. (2014). Estimating Impervious Surface Distributions:; A Comparisonof Object Based Analysis and Spectral Mixture Analysis, University of Salburg/ Austria, pp. 1-5.

[43] Carlson, T. N., Perry, E. M., and Schmugge, T. J. (1990). Remote Estimation of Soil MoistureAvailability and Fractional Vegetation cover for Agricultural fields, Agricultural and Forest Meteorology, Vol. 52, pp. 45–69.

[44] Rincon, D., Khan, U. T., and Armenakis, C. (2018). Flood Risk Mapping using GIS and Multi-Criteria Analysis: a Greater Toronto Area Case Study, Geosciences, Vol. 8, No. 275, pp. 1-27. doi:10.3390/geosciences8080275

[45] Johnson, A. I. (1991). A Field Method for Measurement of Infiltration, Geological Survey Water– Supply Paper 1544 – F, U.S. Geological Survey, pp. 4.

[46] USDA-NRCS, (2004). Soil Infiltration, Soil Health – Guides for Education, pp. 1–7.

[47] Anni, A. H., Cohen, S., and Praskievicz, S. (2020). Sensitivity of Urban Flood Simulations to Stormwater Infrastructure and Soil Infiltration, Journal of Hydrology, No. 588, pp. 1 – 10. https://doi.org/10.1016/j.jhydrol.2020.125028

[48] Martinez, C., Sanchez, A., Vojinovic, Z. and Hernandez, O. (2019). Surface Water InfiltrationBased Approach for Urban Flood Simulations, E- proceedings of the 38th IAHR World Congress September 1-6, 2019, Panama City, Panama, pp. 1176-1185. doi:10.3850/38WC092019-1229

[49] Heywood, I., Cornelius, S., and Carver, S. (2006). An Introduction to Geographic InformationSystem, 3rd Edition, Pearson Education Limited, Edinburgh Gate Harlow Essex CM20 2JE England, pp. 77 – 91, 203.

[50] Zhilin, L., Qing, Z., and Christopher, G. (2005). Digital Terrain Modeling Principles andMethodology, CRC Press, 2000 N. W. Corporate Blvd., Boca Raton, Florida 33431, pp. 59, 236.

[51] Chanthanmas, Y., Anantasuksomsri, S., and Tontisirim, N. (2017). Review of Urban FloodImpact Reduction due to Climate Change Adaptation Driven by Urban Planning Management in Pathumthani Province, Thailand, International Review for Spatial Planning and Sustainable Development, Vol. 5, No. 4, pp. 42 – 53, DOI: http://dx.doi.org/10.14246/irspsd.5.4_42.

[52] Lesslie R.G., Hill M.J., Hill P., Cresswell H.P., Dawson S. (2008). The Application of aSimple Spatial Multi-Criteria Analysis Shell to Natural Resource Management Decision Making. In: Pettit C., Cartwright W., Bishop I., Lowell K., Pullar D., Duncan D. (eds) Landscape Analysis and Visualisation. Lecture Notes in Geoinformation and Cartography. Springer, Berlin, Heidelberg. https://doi.org/10.1007/978-3-540-69168-6_5

[53] Marimuthu, G. and Ramesh, G. (2015). On Moderate Hierarchy Process Pairwise ComparisonModel (Model II), International Journal of Science and Research, Vol. 4, No. 2, pp. 1535-1538.

[54] Joshi, M. M. and Shahapure, S. S. (2015). Study on use of Spatial Multi-criteria Analysis inDecision Making, Journal of Mechanical and Civil Engineering, pp. 6-14.

[55] Saaty, T. L. (1977). A Scaling Method for Priorities in a Hierarchical Structure, Journal ofMathematical Psychology, Vol. 15, pp. 234-281.

[56] Lawal, D. U., Matori, A. N., Yusuf, K. W., Hashim, A. M., and Balogun, A. L. (2014). Analysisof the Flood Extent Extraction Model and the Natural Flood Influencing Factors: A GIS-based and Remote Sensing Analysis, 8th International Symposium of the Digital Earth (ISDES), IOP Conf. Series: Earth and Environmental Science Vol. 18, pp. 1-6.

[57] Yahaya, S. (2008). Multicriteria Analysis for Flood Vulnerability Areas in Hadejia-Jama'AreRiver Basin, Nigeria, ASPRS 2008 Annual Conference Portland, Oregon, April 28 – May 2, 2008, pp. 1-9.

[58] Leopold, L. B. (1968). Hydrology for urban land planning: a guide book on the hydrologic effects of urban land use, U.S. Geological Survey Circular, pp. 554.

[59] Richard, J. U.and Abah, I. A. (2020). Application of Remote Sensing and GeographicInformation (GIS) to Analyze the Impact of Land use on the Wetlands in Port Harcourt and Obio/ Akpor L.G.A. Rivers State, Nigeria, International Journal of Research-Granthaalayah, Vol. 8, No. 05, pp. 355-364. DOI: https://doi.org/10.29121/granthaalayah.v8.i5.2020.242

[60] Tiffany W., Jennifer T., Tom S. Karen C. Anne K., and Dave H., (2006). Direct and Impacts ofUrbanization on Water Quality, Wetlands and Watersheds Article #1, Center for Watersheds Protection, 8390 Main Street, 2nd Floor Ellicott City, MD 21043, pp. 2.

[61] Umaru, E. T. and Adedokun, A. (2020). Geospatial Analysis of Flood Risk and VulnerabilityAssessment along River Benue of Kogi State, Journal of Geographic Information System, Vol. 12, pp. 1-14. https://doi.org/10.4236/jgis.2020.121001

[62] Haider, H. (2019). Climate Change in Nigeria Impacts and Responses, K4D Helpdesk Report,pp. 1-38.

[63] World Bank Group, (2021). Climate Risk Country Profile Nigeria, 1818H Street NW,Washington, DC 20433, pp. 1-36. www.worldbank.org

[64] ESRI, (2008). ArcGIS Spatial Analyst Tutorial, pp. 1 – 64.